brief communication

Frequency domain impedance measurements of erythrocytes

Constant phase angle impedance characteristics and a phase transition

Jian-Zhong Bao,* Christopher C. Davis,* and Robert E. Schmukler‡

*Department of Electrical Engineering and Chemical Physics Program, University of Maryland, College Park, Maryland 20742; and ‡Electrophysics Branch, Center for Devices and Radiological Health, Food and Drug Administration, Rockville, Maryland 20852 USA

ABSTRACT We report measurements of the electrical impedance of human erythrocytes in the frequency range from 1 Hz to 10 MHz, and for temperatures from 4 to 40°C. In order to achieve high sensitivity in this frequency range, we embedded the cells in the pores of a filter, which constrains the current to pass through the cells in the pores. Based on the geometry of the cells embedded in the filter a circuit model is proposed for the cell-filter saline system. A constant phase angle (CPA) element, i.e., an impedance of the form $Z = A/(j\omega)^{\alpha}$, where A is a constant, $j = \sqrt{-1}$, ω is angular frequency, and $0 < \alpha < 1$ has been used to describe the ac response of the interface between the cell surface and the electrolyte solution, i.e., the electrical double layer. The CPA and other elements of the circuit model are determined by a complex nonlinear least squares (CNLS) fit, which simultaneously fits the real and imaginary parts of the experimental data to the circuit model. The specific membrane capacitance is determined to be 0.901 ± 0.036 $\mu F/cm^2$, and the specific cytoplasm conductivity to be 0.413 ± 0.031 S/m at 26°C. The temperature dependence of the cytoplasm conductivity, membrane capacitance, and CPA element has been obtained. The membrane capacitance increases markedly at ~37°C, which suggests a phase transition in the cell membrane.

INTRODUCTION

One approach to understanding the behavior of the cell membrane and cell interior is to study the small electrical signal ac response of the cell by impedance spectroscopy. The electric and dielectric properties of living cells provide information about kinetic processes in the cell membrane and the dynamics of ions and water molecules inside the cells. There have been three common methods for electric and dielectric investigations of biological cells: the suspension method (Schwan, 1957, 1965), the micropipette method (Takashima et al., 1988), and the dielectrophoresis method (Marszalek et al., 1991; Kaler and Jones, 1990); all of these methods have drawbacks and limitations. One of the present authors (Schmukler, 1981) was the first to develop a very sensitive impedance measurement technique, in which cells are embedded in the pores of a Nuclepore filter (Costar Nuclepore, Inc., Cambridge, MA). This method has much higher sensitivity than that of the traditional suspension method in the frequency range <1 MHz, because the filter greatly reduces the shunt current pathway around the cells in the pores, and has a much broader frequency range than that of the micropipette method, which is restricted to the low frequency range <1 kHz because of the large parasitic impedance of the micropipette used (Asami et al., 1990). In fact, our method covers the traditional frequency gap (1 kHz–1 MHz) between the micropipette and the suspension methods. This technique also provides physiological conditions for the cells under measurement compared with the suspension method: where cells are packed very tightly to achieve a high concentration, and a low ionic strength electrolyte solution is used to increase the resistivity of the medium surrounding the cells; and the micropipette method: where the pipette punctures the cell. Another relative advantage of this technique is that because of the well defined geometric form of the cells embedded in filter, the area being measured is more precisely defined such that the interpretation of the experimental data is more accurate.

With this technique we have found that the impedance spectra of human erythrocytes over a wide frequency range (1 Hz–10 MHz) exhibit constant phase angle (CPA) character. With an analogue circuit model based upon the measurement chamber and cell geometry, we can identify the interface between the cell surface and the electrolyte environment as most responsible for this CPA behavior. The CPA impedance element exhibits a power-law function of angular frequency ω, i.e.,

$$Z = \frac{A}{(j\omega)^{\alpha}}, \tag{1}$$

where A is a constant, $j = \sqrt{-1}$, and $0 < \alpha < 1$.

Impedance measurements as a function of temperature strongly suggest that a phase transition occurs in the cell membrane at ~37°C: the marked increase of the membrane capacitance over a small temperature range may be caused by a structural change of the lipid molecules in the membrane. Given the importance of

0006-3495/92/05/1427/08 $2.00

the cell membrane in the functioning of the cell, it may be quite significant that a phase transition occurs so close to physiological temperature.

EXPERIMENT

Human erythrocytes were obtained by finger puncture and washed with saline solution (9 g NaCl/liter). In our saline-filled measurement chamber shown in Fig. 1, which has been described in detail elsewhere (Bao, 1991; Schmukler, 1989), a polycarbonate Nuclepore filter is clamped between the upper and lower halves of the chamber. The cells were layered onto the filter uniformly, and then pushed into the pores of the filter by a small hydrostatic pressure (~ 300 mm H_2O, or 22 mm Hg), because red cells are very flexible. Enough time (~ 2 h) is allowed to permit cells to fill almost all the pores of the filter, and measurements are not performed until fluid flow through the chamber has stopped. The four-electrode technique we use avoids distortion of the impedance data by the electrode–electrolyte interface polarization at the two current input electrodes (porous carbon). Polarization at the voltage measurement electrodes (porous tantalum prepared from pressed powder) was minimized because of the very small current going through these electrodes and their very large surface area. Chamber temperature is controlled by a Polyscience 9500 high speed constant temperature circulator (Polyscience Co., Niles, IL) and monitored with a YSI series 500 thermocouple (Yellow Springs Instrument Co., Yellow Springs, OH) to ensure its stability during each frequency sweep. The core instrument is a Solartron 1260 Impedance Analyzer (Schlumberger Instruments, Hampshire, England), which is controlled by a PC (AST 286/12 MHz). The amplitude of the generator output of the analyzer was set at only 10 mV, which gives a voltage drop cross the filter of less than 3 mV, which is a relatively small perturbation on the static membrane potential (13 mV) (Lassen, 1977). Both voltage and current measurement channels of the analyzer are ac coupled to reduce electrode polarization effects. Preparation of samples and setting up of the experiment is conducted at room temperature. Once the cells are well embedded in the filter, the temperature is lowered to 4°C. At each subsequent temperature point ~ 30 min is allowed to permit cells and chamber to reach thermal equilibrium.

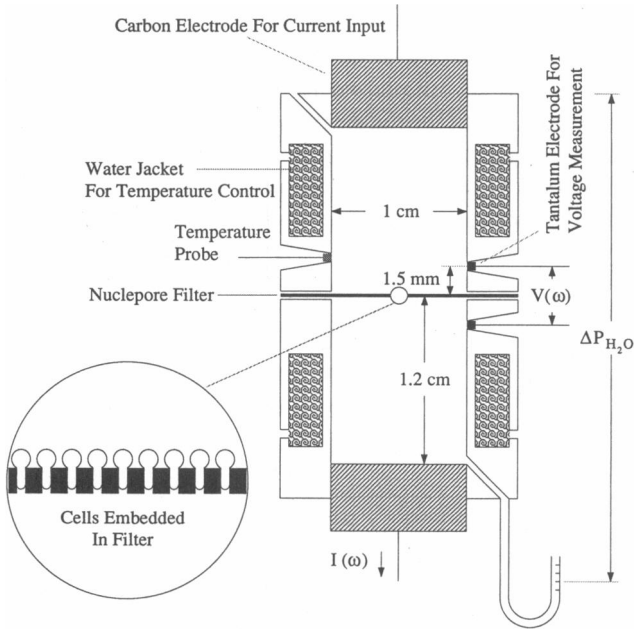

FIGURE 1 Electrical impedance measurement chamber.

Circuit model

A cell embedded in a pore of the filter is depicted schematically in Fig. 2 *a*. Because all the cells embedded in the filter are approximately equivalent and in parallel, we can use a simple circuit based on the geometric form of the embedded cell in this diagram to model the whole cell-filter-saline system. To obtain background impedance values, the impedance spectra of both saline alone and saline with a

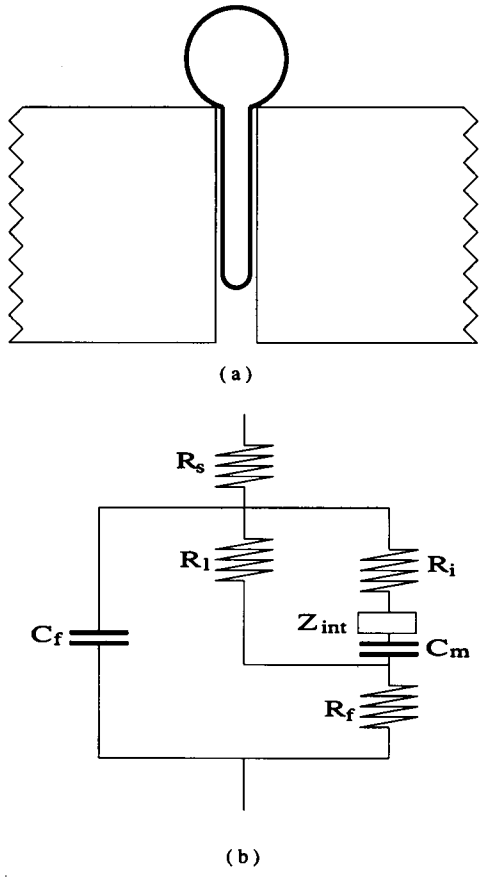

FIGURE 2 (*a*) A human erythrocyte embedded in a pore of a polycarbonate filter, where the cell is in a well defined geometric state. (*b*) The circuit model for the cell-filter saline system based on the geometry of the cell in *a*, where R_s is the bulk resistance of the saline solution, R_l is the leak resistance around the cells embedded in the filter, R_i is the cytoplasm resistance of the cells, C_m is the membrane capacitance of the cells, Z_{int} is the interface impedance (CPA element) between the cell surface and saline solution, C_f is the filter capacitance, and R_f is the resistance due to the unfilled part of the pores of the filter because the cells do not completely penetrate the pores, so it should only be a fraction of the filter resistance before the cells are introduced into the chamber.

filter clamped in the chamber were taken before measurements on the erythrocytes. A typical group of impedance spectra are shown in Fig. 3. The spectra of erythrocytes clearly show a dispersion at ~200 kHz, which we have determined cannot be described in terms of a finite, resolvable set of frequency-independent RC elements, no matter how these are chosen. However, these spectra are consistent with the circuit model in Fig. 2 *b*, in which Z_{int} is a CPA element. Both cytoplasm resistance (R_i) and membrane capacitance (C_m) are treated as frequency-independent elements. The dc pathway through the membrane was ignored, because its resistance is at least three orders of magnitude larger than the leak resistance (R_l) around the cells (Schmukler, 1989).

Complex nonlinear least squares (CNLS) fit

In CNLS the objective function S is given by

$$S = \sum_{n=1}^{N} \{W_r(\omega_n)\,[Z^r_{\text{model}}(\omega_n, \vec{P}) - Z^r_{\text{exp}}(\omega_n)]^2 + W_i(\omega_n)[Z^i_{\text{model}}(\omega_n, \vec{P}) - Z^i_{\text{exp}}(\omega_n)]^2\}, \quad (2)$$

where N is the number of data points, the ω_n are the frequency points, subscript and superscript r and i denote the real and imaginary parts, respectively, W is the weighting factor, Z_{model} is the analytical complex impedance expression of the circuit model, $\vec{P} = \{P_1, \ldots, P_k\}$ are k real parameters of the model, and Z_{exp} is the experimental data. Because both real and imaginary parts are taken into account in Eq. 2, CNLS simultaneously fits both parts of the complex impedance data to the circuit model, which ensures a complete fit. The best-fit values of these parameters and their confidence limits are evaluated by minimizing S using the Marquardt algorithm (Press et al., 1988).

RESULTS AND DISCUSSION

The experimental data obtained at each temperature could always be well fitted to the circuit model shown in Fig. 2 *b* by means of a CNLS fit. We use the spectra of erythrocytes in Fig. 3 for a CNLS fit as shown in Fig. 4. The circuit parameters, which reflect the response of the

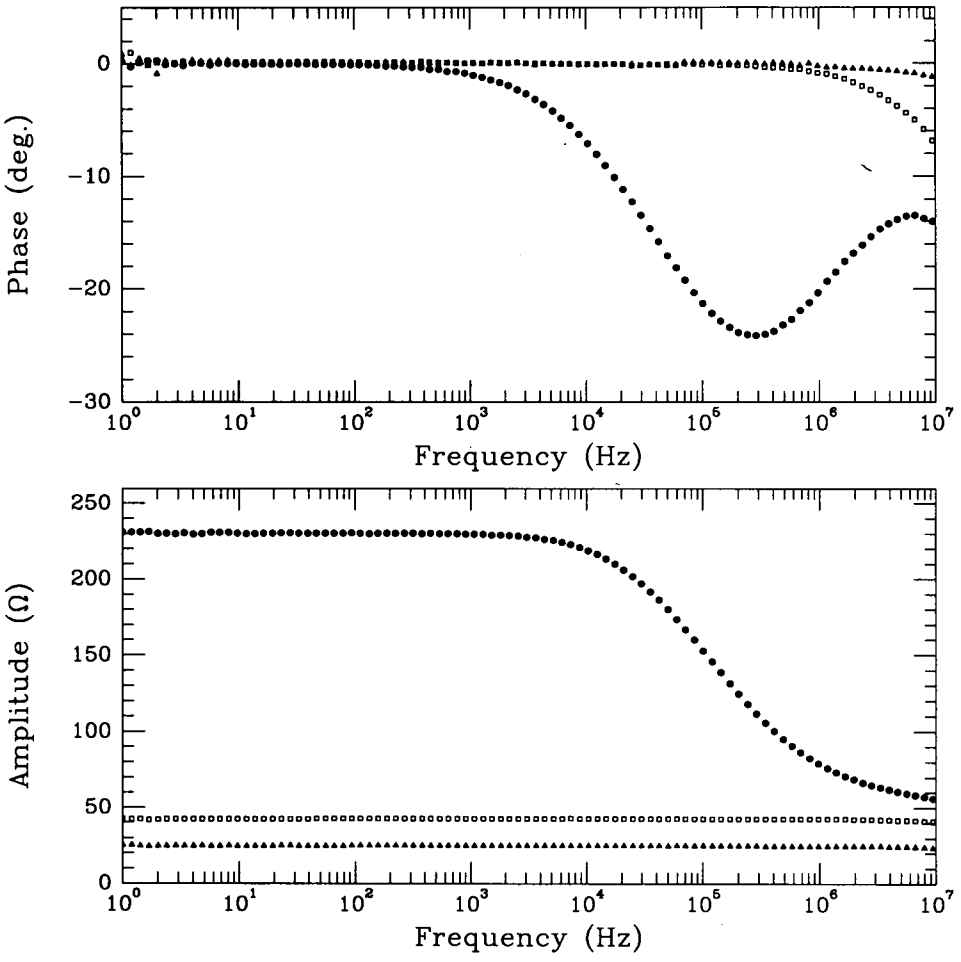

FIGURE 3 Comparison of the spectra of saline alone (▲), saline with a filter (□), and erythrocytes embedded in the filter (●). The difference between the spectra of saline with a filter and the spectra of saline alone gives the filter resistance before cells are introduced, which is ~17 Ω. The spectra are taken at 26°C.

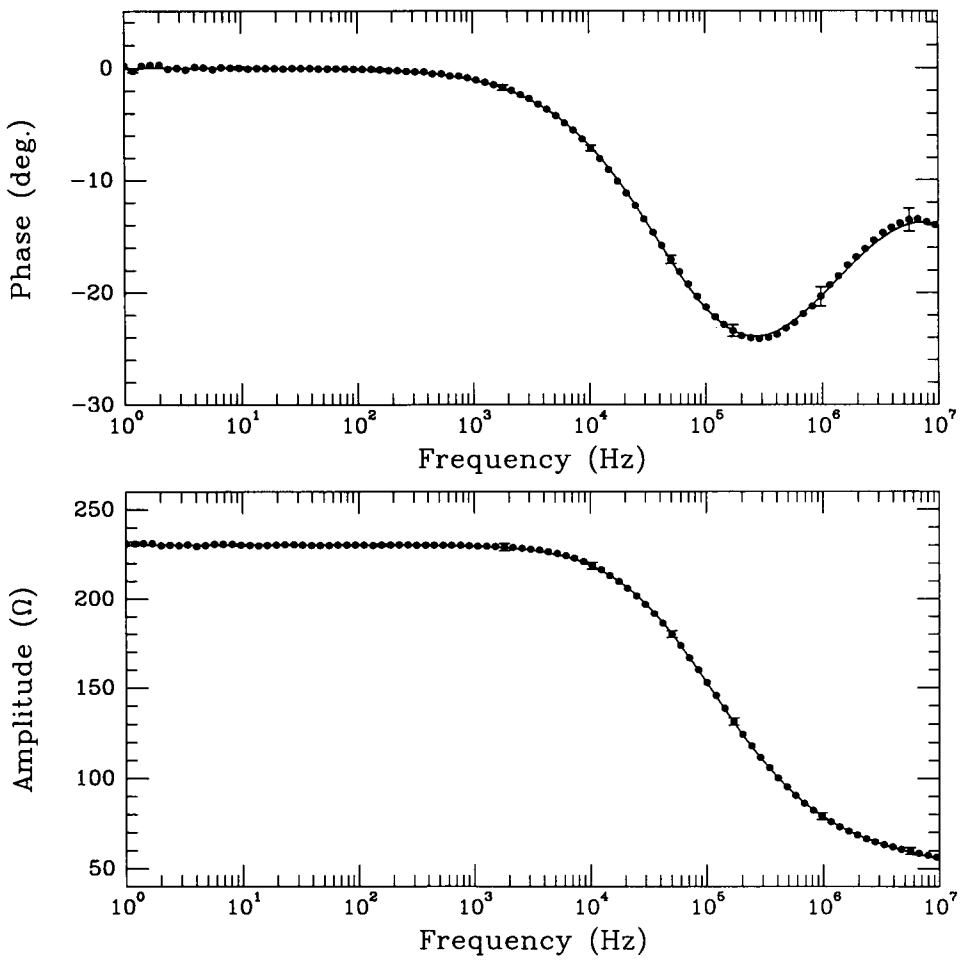

FIGURE 4 A typical CNLS fit (*solid line*) of the experimental data (●) of erythrocytes embedded in a filter to the circuit model shown in Fig. 2 *b*. The spectra are taken at 26°C.

whole cell-filter-saline system, found from this typical data fit at 26°C are shown in Table 1.

After converting α, A, and R_i, using the filter characteristics (pore density = $4.22 \times 10^9/m^2$, pore diameter = 2.05 μm, and filter thickness = 13.15 μm), we get the averages of these parameters for a single cell: CPA element exponent (α) = 0.582 ± 0.088, CPA element constant (A) ($\times 10^{11}$/cell) = 1.346 ± 0.173, and leak resistance around a cell = 66.53 ± 0.19 MΩ. Conversion of C_m and R_i to specific membrane capacitance and specific cytoplasm conductivity, respectively, is based upon the geometric state of the embedded cell, as shown in Fig. 2 *a*. The size of the surface area is important in determining the accuracy of the specific membrane capacitance, so we take both the top (almost) sphere and bottom hemisphere into account although the contribution from the top sphere is much smaller than that of the bottom hemisphere. In the calculation of the specific cytoplasm conductivity we only consider the major contribution to R_i, which results from the cytoplasm in the part of the cell that is extruded into the pores of the filter. It is more difficult to calculate the contribution from the cytoplasm within top sphere, which in fact contributes much less resistance. The specific cytoplasm conductivity calculated in this way will give a slightly smaller value. The average specific membrane capacitance and specific cytoplasm conductivity from five

TABLE 1 Circuit parameters found from CNLS fit, which is graphically displayed in Fig. 4.

C_m = 21.67 ± 0.83 nF	R_i = 25.81 ± 1.28 Ω
α = 0.582 ± 0.088	A = 406.11 × 10^3 ± 52.35 × 10^3
R_l = 200.74 ± 0.56 Ω	R_f = 4.90 ± 3.37 Ω
R_s = 24.64 ± 3.33 Ω)	C_f = 109.64 ± 26.68 pF

experiments at 26°C and a comparison with results from other methods are shown in Table 2.

Our results yield values for specific membrane capacitance that are in very good agreement with those of other methods. The value for the specific cytoplasm conductivity is relatively smaller than that found with suspension methods. This difference may be the result for three reasons: (*a*) our method actually measures the ohmic current flowing through the cytoplasm, whereas in the suspension method the conductivity is calculated, in a very model-dependent way, from the dielectric loss, which can be treated as resulting from an equivalent conductivity that increases with frequency. This may partially explain a higher conductivity being found by a suspension method at 90 MHz than by our direct method at lower frequencies (1 Hz–10 MHz); (*b*) as mentioned earlier, ignoring the cell sphere outside each pore results in a smaller specific cytoplasm conductivity; and (*c*) R_i in the circuit model is mainly determined by data in the high frequency range of our measurements such that the accuracy of R_i is relatively lower than that of C_m. However, our results suggest a value for the specific cytoplasm conductivity at low frequencies, a parameter that cannot be obtained with the suspension method. In addition, our experiments suggest that the interface between the cell surface and the electrolyte is responsible for the fractional power law frequency dispersion that is described as a CPA element. The frequency profile of impedance spectra we observed is a bulk response of the whole cell-filter-saline system. In our circuit model, the frequency and shape of dispersion is mainly due to the membrane capacitance, cytoplasm resistance, leak resistance, and interface CPA element. In the CNLS fit all the circuit elements are treated independently, and their best-fit values are determined not only by dispersion frequency but, more importantly, dispersion shape also. The estimated values of R_s and R_f, which can also be obtained from the background spectra, are used as a reliability check of the circuit model as well as the CNLS fit. Our results show that they are in good agreement, and the cell membrane can be treated just as an ideal frequency-independent capacitor in this frequency range.

TABLE 2 Comparison of the results from different methods

Erythrocyte parameters	Filter embedding method‡	Suspension method	Micropipette method
Specific membrane capacitance ($\mu F/cm^2$)	0.901 ± 0.036	0.853 ± 0.029*	0.89 ± 0.16*
Specific cytoplasm conductivity (S/m)	0.413 ± 0.031	0.518 ± 0.007§	n.d.

‡Obtained in the frequency range (1 Hz–10 MHz) at 26°C; *(Takashima et al., 1988); §at 90 MHz (Pauly and Schwan, 1966).

The CPA element is an empirical impedance function, a complex power-law function of frequency, yet has proven to be of considerable value in data fitting. Many types of systems exhibit a region of such behavior, and recent explanations of this phenomenon have been based on a presumed self similarity in the structure of the system or in its relaxation dynamics (Dissado and Hill, 1988; Kaplan and Gray, 1985; Liu, 1985). In the electrolyte-electrode system the ac interface response can be represented by a fractal circuit, which will reduce to a CPA element at low frequencies. A relationship between the fractal dimension of the interface and the exponent α of such a CPA element has been established (Liu, 1985). Technically, the potential of the surface of the electrode is set to ground in the derivation. This is acceptable for an electrode but not for an insulator. At the interface, a charge double layer will be formed in the electrolyte solution for both electrolyte-electrode and electrolyte-insulator cases, however, there is some free charge accumulation on the electrode along the interface, which is not the case for an insulator because of its lack of free charges. This is the major difference between these two systems, which makes studies of the interface CPA element in electrolyte-insulator system much more difficult.

From the circuit model, the natural explanation for the origin of the CPA element is the interface between the cell surface and surrounding electrolyte, but this interface may not offer the only explanation. Electron micrographs reveal that each cell embedded in the pore has a slightly different penetration length, each pore makes a slightly different angle with the filter surface, and the pore diameters are slightly different. These differences can lead to different time constants, and it is well known that a distribution of time constants also gives CPA behavior (Raistrick, 1987; Schwan, 1957).

The temperature dependence of cell parameters is shown in Fig. 5. It is clear from Fig. 5 *a* that the frequency exponent α increases linearly with increasing temperature, which is different from its behavior in the electrolyte-electrode system, where it is found that the exponent decreases with increasing temperature (Bates et al., 1986). Generally the exponent α is intimately related to the microstructure of the interface, although an analytical relation between these has not been found. An increasing value of α suggests that the surface of the cell may be becoming increasingly smooth. Fig. 5 *b* shows that the constant of the CPA element increases nonlinearly with temperature. So far, attention to the CPA element has focused only on the frequency expo-

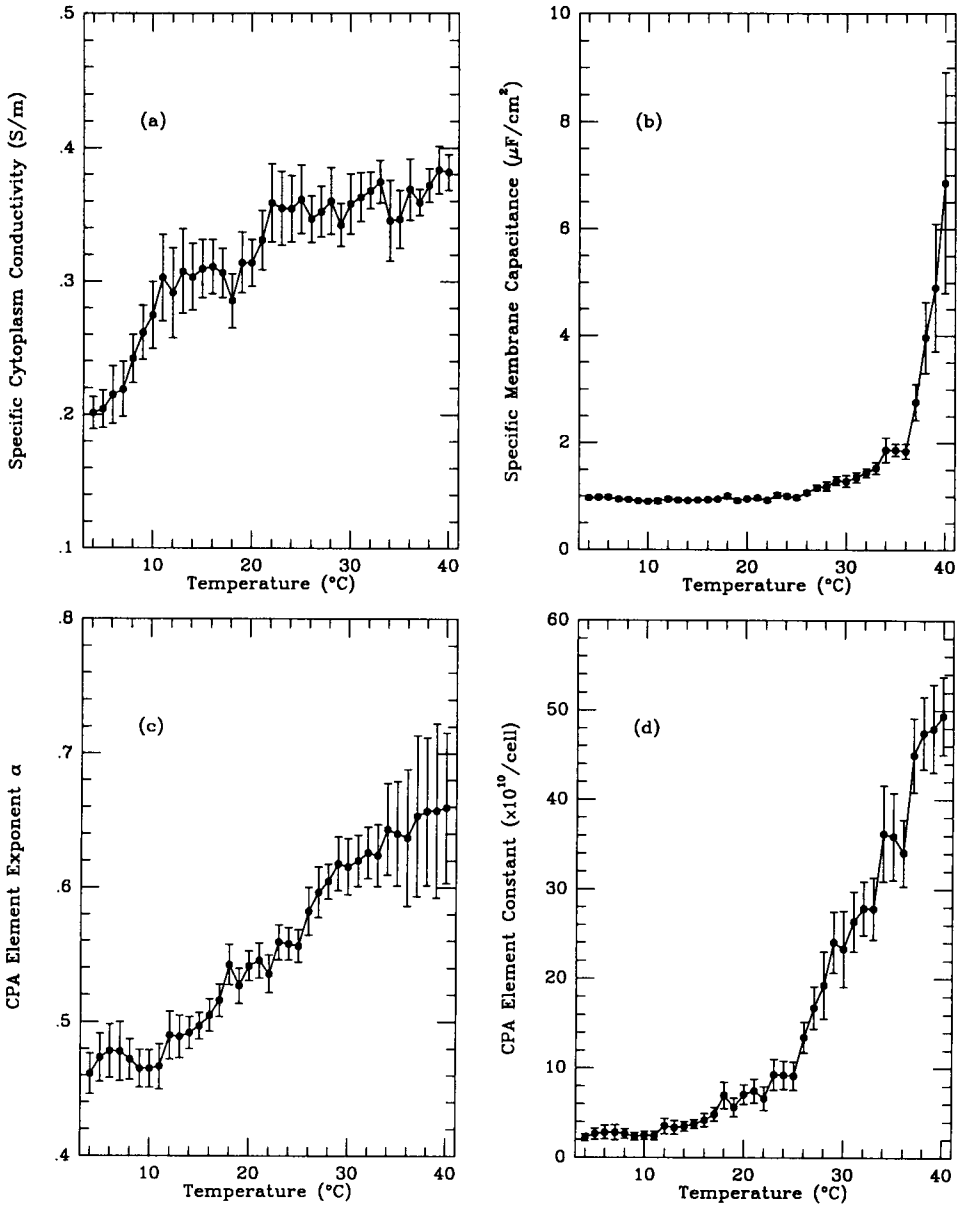

FIGURE 5 Temperature dependence of specific cytoplasm conductivity, specific membrane capacitance, and CPA element of human erythrocytes. The frequency range of the spectra yielding above cell parameters is from 1 Hz to 10 MHz.

nent α, the physical meaning of the constant A is still unclear, except for a few systems, such as the Warburg impedance (Raistrick, 1987), which is a typical example of a CPA element. The Warburg impedance is obtained from the solution of the one-dimensional diffusion equation for a particle in a semi-infinite space, a situation mathematically analogous to an RC transmission line (Raistrick, 1987). The exponent (α) of the Warburg impedance is equal to one-half, and the constant (A) relates to the diffusion coefficient, the concentration in the bulk, and the valence number of the diffusing charged particles and the temperature.

Measurement of the cytoplasm conductivity at low frequencies is difficult because of the highly insulating surrounding membrane. The technique used here allows us to perform this measurement without lysing the cells. Low frequency data on the cytoplasm conductivity might be helpful in assessing the biological effect of extremely low frequency (ELF) radiation, which is a matter of current concern to many people. The temperature

dependence of the interior conductivity is given in Fig. 5 *c*. This conductivity results largely from its free ion and water content. The ion content consists primarily of K^+, Na^+, Mg^{++}, Cl^-, and HCO_3^- ions. If the relative ion and water concentrations in the cytoplasm are known, then the conductivity values give information about the state of these ions and water molecules, for example, whether they are bound or not. The uneven curve of the temperature dependence of the cytoplasm conductivity may be partially attributed to the release of bound water molecules and ions from hemoglobin molecules and membranes.

Much evidence from x-ray diffraction (Wack and Webb, 1988) and other studies has shown that there are three different common structural states for some fully hydrated lipid bilayer systems. For dipalmitoylphosphatidylcholine (DPPC), in the temperature range lower than 34°C (T_p), the hydrocarbons of the lipid molecules form a solid phase ($L_{\beta'}$) with stiff extended chains in a hexagonal lattice. At temperatures higher than 42°C (T_m), they become disordered into a more liquid-like phase ($L_{\alpha'}$) (Yang and Nagle, 1988; Nagle, 1980). Between these two phases, there is a structurally modulated or "rippled" phase ($P_{\beta'}$). NMR studies (Wittebort et al., 1981) show that the $P_{\beta'}$ phase is a coexistence domain of $L_{\beta'}$ and $L_{\alpha'}$. When the lipid bilayer undergoes the transition $L_{\beta'} \rightarrow P_{\beta'}$ ("pretransition"), the hydrocarbon chains are partially melted, the surface of the membrane becomes rippled, the effective surface area increases, and the average thickness of the bilayer decreases. When it undergoes the transition $P_{\beta'} \rightarrow L_{\alpha'}$ ("main" transition), the hydrocarbon chains are completely melted, the lateral spacing of the lipid molecules increases, the thickness of the bilayer decreases, and the surfaces of the bilayer become flat again. The transition temperatures (T_p and T_m) are systematically increasing, and the temperature range for the $P_{\beta'}$ phase ($T_m - T_p$) decreasing with chain length (N_c) increasing. Phase transitions of biomembranes are not documented as well as those of lipid membrane because of the complexity of the biomembrane, which contains many other molecules such as proteins. The interaction between these molecules will limit the mobility of the lipid molecules and affect the phase transition such that their structural configurations may be quite different from, and more complicated than, those of pure lipid membranes. However, because the major constituents of the biomembrane are lipid molecules, the properties of a biomembrane will more or less reflect those of a lipid bilayer. A well documented case of a biomembrane structural phase transition is in Acholeplasma Laidlwii (Engelman, 1970), which is a primitive organism where x-ray diffraction studies have shown that a gradual structural phase transition occurs in the cell membrane as its temperature is changed, and the transition temperature varies with the composition of the membrane. Our measurements show that the membrane capacitance of the human erythrocyte stays constant as long as the temperature is below 30°C, which is consistent with earlier work (Schwan and Li, 1953), and increases rapidly at ~37°C over a small temperature range by several-fold compared with that at low temperatures. This is very surprising and has not been previously reported for mammalian cell membranes. The substantial increase in membrane capacitance may result from an increase in the surface area because the surface has become "rippled" where we are presuming that a "rippled" phase also exists for biomembranes or from a decrease in the thickness of the membrane. However, it is unreasonable to ascribe all the increase in membrane capacitance to a reduction in thickness. A more plausible explanation for an increasing specific membrane capacitance is the dielectric constant of the membrane. Water can diffuse through the cell membrane very effectively when the membrane is in the fluid phase. The permeability is on the order of 10^{-3} cm/s, which is three orders higher than that in the gel phase. A large permeability jump, which might result from critical fluctuations, at the phase transition temperature has been found (Cevc and Marsh, 1987). Water transport is controlled by the diffusion of conformational chain defects, which are responsible both for the formation of the free volume allowing the insertion of small molecules, such as water, and for the driving force for transport along the direction of the chains. If the number of these defects increases during the phase transition (Sackmann, 1983), then the participant number of water molecules in the cell membrane should also increase. The dielectric constants for free and bound water are ~80 and 10, respectively, in this frequency range, much higher than that of the cell membrane, which is ~3, such that the effective dielectric constant of the cell membrane increases greatly during the phase transition. Although we cannot directly compare our results with any existing theories, or even experimental results, an increasing membrane capacitance is consistent with the structural change in lipid bilayers and the increase of effective dielectric constant of the cell membrane during a phase transition. Our ability to see this phenomenon, compared with suspension methods, may come from (*a*) our sensitive analysis of both amplitude and phase in our impedance spectra; (*b*) physiological conditions under which our measurements are performed.

Although the values for the specific membrane capacitance at high temperatures are subject to relatively large errors, which may arise from the variability of the state of the membrane near the phase transition, the

phase transition effect in the cell membrane is still obvious. Certain transport processes, such as diffusion across the membrane, are particularly effective when the crystalline and liquid domains coexist. Erythrocytes play a central role in the transport of respiratory gases, and effective diffusion processes in the membranes are critical. High molecular mobility is required for a multitude of transport processes of importance in active membranes, so it is perhaps not accidental that the phase transition we observed occurs near physiological temperature.

In summary, the results of this research demonstrate the promise of the technique of embedding cells in a filter as an experimental tool for basic studies of the electric and dielectric properties of biological cells and their membranes, which complement suspension, micropipette, and dielectrophoresis methods. Furthermore, the interface between the cell surface and the electrolyte environment plays an important role in impedance dispersion, and using a CPA element to describe it may offer a new way to understand the interaction between cells and their surrounding environment. Furthermore, the membrane capacitance increase markedly at ~37°C, which suggests a phase transition in the cell membrane. A phase transition near physiological temperature may not only be a physical phenomena of abstract interest, but may have real biological significance.

We are grateful to Mays Swicord for his help. This work is from a dissertation submitted to the Graduate School of the University of Maryland at College Park by Jian-Zhong Bao in partial fulfillment of the requirements for the Ph.D. degree in Chemical Physics.

This work was supported by FDA/CDRH through contract No. 223-84-6038.

The mention of commercial products, their sources, or their use in connection with material reported herein is not to be construed as either an implied or actual endorsement of such products by the Department of Health and Human Services.

Received for publication 22 August 1991 and in final form 23 December 1991.

REFERENCES

Asami, K., Y. Takahashi, and S. Takashima. 1990. Frequency domain analysis of membrane capacitance of cultured cells (HeLa and myeloma) using the micropipette technique. *Biophys. J.* 58:143–148.

Bao, J. Z. 1991. Impedance spectroscopy of human erythrocytes: constant phase angle characteristics and a membrane phase transition. Ph.D. thesis. University of Maryland.

Bates, J. B., J. C. Wang, and Y. T. Chu. 1986. Impedance of metal-solid electrolyte interfaces. *Solid State Ionics.* 18, 19:1045–1049.

Cevc, G., and D. Marsh. 1987. Phospholipid Bilayers. John Wiley and Sons, New York.

Dissado, L. A., and R. W. Hill. 1988. Constant-phase-angle and power-law regimes in the frequency response of a general determinate fractal circuit. *Phys. Rev.* B37:3434–3439.

Engelman, D. M. 1970. X-ray diffraction studies of phase transition in the membrane of Mycoplasma laidlawii. *J. Mol. Biol.* 47:115–117.

Kaler, K. V. I. S., and T. B. Jones. 1990. Dielectrophoretic spectra of single cells determined by feedback-controlled levitation. *Biophys. J.* 57:173–183.

Kaplan, T., and L. J. Gray. 1985. Effect of disorder on a fractal model for the ac response of a rough interface. *Phys. Rev.* B32:7360–7366.

Lassen, U. V. 1977. Electrical potential and conductance of the red cell membrane. *In* Membrane Transport in Red Cells. J. Ellory and V. Lew, editors. Academic Press, New York. 137–174.

Liu, S. H. 1985. Fractal model for the ac response of a rough interface. *Phys. Rev. Lett.* 55:529–532.

Marszalek, P., J. J. Zielinsky, M. Fikus, and T. Y. Tsong. 1991. Determination of electric parameters of cell membrane by a dielectrophoresis method. *Biophys. J.* 59:682–687.

Nagle, J. F. 1980. Theory of the main lipid bilayer phase transition. *Annu. Rev. Phys. Chem.* 31:157–195.

Pauly, H., and H. P. Schwan. 1966. Dielectric properties and ion mobility in erythrocytes. *Biophys. J.* 6:621–639.

Press, W. H., B. P. Flannery, S. A. Teukolsky, and W. T. Vetterling. 1988. Numerical Recipes in C. Cambridge University Press, Cambridge, U.K.

Raistrick, I. D. 1987. Chapter 2 Theory. *In* Impedance Spectroscopy. J. R. Macdonald, editor. J. Wiley and Sons, New York. 27–132.

Sackmann, E. 1983. Physical foundations of the molecular organization and dynamics of membranes. *In* Biophysics. W. Hoppe, W. Lonhmann, H. Marki, and H. Ziegler, editors. Springer, New York.

Schann, O. F., and Ruiz-Ceretti. 1978. Impedance Measurements in Biological Cells. J. Wiley and Sons, New York. p. 137.

Schmukler, R. 1989. Measurements of the electrical impedance of living cells in frequency domain. *In* Charge and Field Effects in Biosystems—2. M. J. Allen, S. F. Cleary, and F. M. Hawkridge, editors. Plenum Press, New York. 357–372.

Schmukler, R. 1981. A new technique for impedance measurements of isolated cells. E.Sc.D. Thesis. Columbia University, New York.

Schwan, H. P. 1965. Determination of biological impedance. *In* Physical technique in biological research. W. L. Nastuk, editor. Academic Press, New York. 323–407.

Schwan, H. P. 1957. Electrical properties of tissue and cell suspensions. *In* Advances in Biological and Medical Physics. J. H. Lawrence and C. A. Tobias, editors. Academic Press, New York. 147–209.

Schwan, H. P., and K. Li. 1953. Capacity and conductivity of body tissues at ultrahigh frequencies. Proc. I.R.E. 41:1735–1740.

Takashima, S., K. Asami, and Y. Takahashi. 1988. Frequency domain studies of impedance characteristics of biological cells using micropipette technique. *Biophys. J.* 54:995–1000.

Wack, D. C., and W. W. Webb. 1988. Measurements of modulated lamellar $P_{\beta'}$ phase of interacting lipid membranes. *Phys. Rev. Lett.* 61:1210–1213.

Wittebort, R. J., C. F. Schmidt, and R. G. Griffin. 1981. Solid-state carbon-13 nuclear magnetic resonance of the lecithin gel to liquid-crystalline phase transition. *Biochemistry.* 20:4223–4228.

Yang, C. P., and J. F. Nagle. 1988. Phase transformations in lipids follow classical kinetics with small fractional dimensionalities. *Phys. Rev.* A37:3993–4000.